

Impact of the tip radius on the lateral resolution in piezoresponse force microscopy

T Jungk¹, Á Hoffmann and E Soergel

Institute of Physics, University of Bonn, Wegelerstraße 8,
53115 Bonn, Germany
E-mail: jungk@uni-bonn.de

New Journal of Physics **10** (2008) 013019 (9pp)

Received 21 June 2007

Published 21 January 2008

Online at <http://www.njp.org/>

doi:10.1088/1367-2630/10/1/013019

Abstract. We present a quantitative investigation of the impact of tip radius as well as sample type and thickness on the lateral resolution in piezoresponse force microscopy (PFM) investigating bulk single crystals. The observed linear dependence of the apparent width of a ferroelectric domain wall on the tip radius as well as the independence of the lateral resolution on the specific crystal-type are validated by a simple model. Using a Ti–Pt coated tip with a nominal radius of 15 nm the so far highest lateral resolution in bulk crystals of only 17 nm was obtained.

Contents

1. Introduction	2
2. Experimental	2
2.1. Tip specifications	3
2.2. Sample specifications	3
3. Theoretical model	3
4. Experimental results	5
4.1. Dependence on the tip radius	5
4.2. Dependence on the sample thickness	6
4.3. Dependence on the sample type	7
5. Conclusions	8
Acknowledgments	8
References	8

¹ Author to whom any correspondence should be addressed.

1. Introduction

Ferroelectrics attract increasing attention due to their applicability, e.g. for electrically controlled optical elements [1], for efficient frequency-doubling [2, 3], for photonic crystals [4], or for non-volatile memories with an otherwise un-reached data-storage density [5]. The size of the domain structures required for these applications varies from a few microns down to some nanometres. The smaller the domains are, the more the properties of the domain walls become important. Generally, the width of the domain walls is expected to be a few crystal lattice cells [6]–[8]. Measuring the birefringence with scanning near-field microscopy in LiTaO₃, however, showed a distortion of the crystal over a width of 3 μm across the domain boundary [9]. Detecting the Raman modes with a confocal defect-luminescence microscope, an influence of the domain wall in LiNbO₃ further than 1 μm into the surrounding material was observed [10]. On the other hand, high-resolution transmission electron microscopy yielded a domain wall width in PbTiO₃ of <2.8 nm [11] and with scanning nonlinear dielectric microscopy, a width of only 0.5 nm in ultra-thin PbZrTiO₃ films was determined [12].

In the past ten years, piezoresponse force microscopy (PFM) has become a very common technique for domain imaging mainly due to its high lateral resolution without any need for specific sample preparation. This technique is based on the fact that ferroelectric materials are necessarily piezoelectric [13]. Therefore, the application of voltages causes thickness changes of the sample via the converse piezoelectric effect. For PFM a scanning force microscope is operated in contact mode with an alternating voltage U_{tip} of frequency f applied to the tip. The periodic thickness changes of the sample and thus the resulting vibrations of the surface are followed by the tip which in turn lead to oscillations of the cantilever that can be read-out with a lock-in amplifier [14, 15]. Neither the amplitude nor the frequency of the applied voltage have a direct influence on PFM imaging. Typically 1–10 V are applied to the tip. The frequency, however, must be chosen high enough to avoid a compensation of the cantilever oscillation by the feedback circuit. The latter can at most respond in the few kiloHertz regime.

PFM imaging is usually influenced by a system inherent background [16]. One consequence is a pretended broadening of the apparent domain wall width W in PFM imaging when using the magnitude output R of the lock-in amplifier for read-out [17]. To obtain reliable data for W we used the in-phase output X of the lock-in amplifier (in the following denoted as PFM signal).

In this contribution, we present a study of the influence of the tip radius on the PFM imaging of 180° ferroelectric domain walls in bulk single crystals. Therefore, we determined the apparent width W of the domain walls when imaged by PFM on LiNbO₃ crystals for tips of different radii. Furthermore we performed a series of measurements with LiNbO₃ samples of different thicknesses. We also compared W for different types of crystals using one unique tip. Finally, we present a simple analytical model that explains the observed dependencies of the apparent domain wall width W on the tip radius, the crystal thickness and the type of sample.

2. Experimental

The experiments were carried out with a commercial scanning force microscope (SMENA from NT-MDT). The system was modified to allow application of voltages to the tip in order to enable PFM measurements. The alternating voltage ($U_{\text{tip}} = 10 \text{ V}_{\text{pp}}$, $f = 30\text{--}60 \text{ kHz}$) was applied to the tip and the backside of the samples was grounded.

Table 1. Specifications of the tips utilized for the PFM measurements.

Label	Manufacturer	Model	Tip radius (nm)	Coating
A	NT-MDT	NSG11	10	–
B	Veeco	OSCM-PT	15	Ti–Pt
C	Veeco	SCM-PIT	20	Pt–Ir
D	MikroMash	NSC35	35	Ti–Pt
E	MikroMash	NSC35	50	Cr–Au
F	NT-MDT	DCP11	50–70	diamond
G	MikroMash	NSC35	90	Co–Cr

2.1. Tip specifications

We used a series of different tips with radii varying from 10–90 nm, classified in table 1. All tips were made out of highly n-doped silicon and conductively coated with different materials. The spring constants ranged from 3 to 70 N m⁻¹. The tip with the smallest radius ($r = 10$ nm) was an exception since it was uncoated. Due to oxidation the outer few nanometres of the surface are modified to a non-conductive SiO₂ layer. As a consequence, the mechanical and the electrical tip do not coincide any more; the SiO₂ layer acts as a dielectric gap between the tip and the sample.

2.2. Sample specifications

The experiments for determining the dependence of the apparent domain wall width W on the tip radius r were performed using periodically poled lithium niobate (PPLN) crystals (period length $\Lambda = 30$ μ m) of 500 μ m thickness. For the measurements of the dependence of W on the sample thickness t we used the same PPLN samples, mechanically thinned by polishing to the thickness wanted (15–1000 μ m). The thinnest sample (0.9 μ m) was a stoichiometric LiNbO₃ crystal. Here, the domains were generated with the help of the tip by applying a voltage of 20 V for 10 min. We also measured a series of samples different from LiNbO₃ as listed in table 2. Those samples had thicknesses of 0.5–2 mm and were either periodically poled (KTiOPO₄ and LiNbO₃) or had arbitrary domain patterns (BaTiO₃, KNbO₃, LiTaO₃, Pb₅Ge₃O₁₁ and SBN).

3. Theoretical model

Calculating the spatial resolution achievable with PFM requires the exact electric field distribution underneath the tip and the electromechanical answer of the material. The latter is given by the dielectric constants as well as the elastic and piezoelectric tensors, respectively. This complex problem is most suitable for the finite element method, where all material constants can be included thus yielding quantitative results [18]. A detailed study on domain wall width imaged by PFM including finite element calculations has recently been undertaken [19]. In this contribution, we propose a much simplified approach to the problem of lateral resolution in PFM. This model is not capable of giving the amplitude of the measured PFM signals because the signals were normalized in order to facilitate the calculations. The

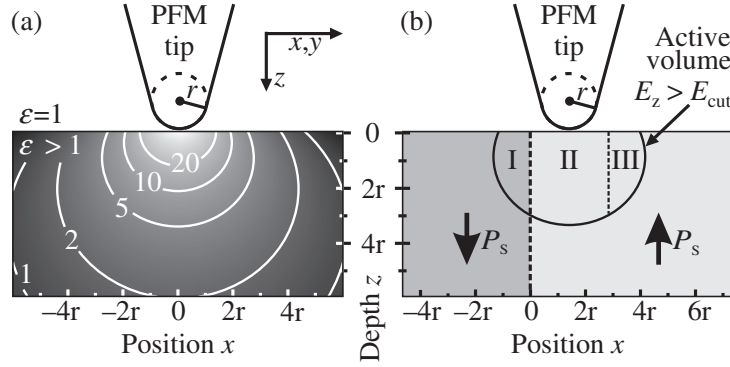


Figure 1. (a) Electrical field distribution E_z underneath a tip of radius r calculated with equation (1) for a sample of infinite thickness. The white lines indicate the shells where the electric field has decayed to the indicated %-value of the maximum electric field E_{\max} present underneath the tip apex. (b) Schematics of the analytical model with the tip in the vicinity of a domain wall. The active volume where $E_z > E_{\text{cut}} \approx 0.05 E_{\max}$ underneath the tip covers both domains. The contributions of part I and III cancel out each other. The resulting surface deformation is thus determined by part II only. P_s denotes the orientation of the spontaneous polarization.

model, however, can give a quantitative prediction of the apparent domain wall width W as a function of the tip radius r and the sample thickness t .

In a first step, the problem was simplified by approximating the spherical apex of the tip with radius r by a point charge q at the distance r above the sample surface. We further assumed the sample to be isotropic with an effective dielectric constant $\epsilon_{\text{eff}} = \sqrt{\epsilon_r \epsilon_z}$ where ϵ_z being the dielectric constant in z -direction and ϵ_r the radial one perpendicular to z . For LiNbO_3 $\epsilon_z = 27.8$, $\epsilon_r = 84.5$ and thus $\epsilon_{\text{eff}} = 48.4$ [20]. Taking the finite thickness t of an isotropic sample into account the relevant electric field component E_z underneath the tip is given by [21]:

$$E_z(x, y, z) = \frac{q}{\epsilon_{\text{eff}}} \left\{ \frac{z+r}{[x^2 + y^2 + (z+r)^2]^{3/2}} + \frac{z-r-2t}{[x^2 + y^2 + (z-2t-r)^2]^{3/2}} \right\}. \quad (1)$$

Next, we define E_{\max} as the maximum electric field underneath the tip apex inside the sample (at $x = y = z = 0$). E_{\max} will be used to normalize the electric field. Furthermore, we scale all lengths with the tip radius r . Thus, the problem has become dimensionless. Figure 1(a) shows the electric field distribution E_z inside a sample of infinite thickness. It can be seen, that at a depth of twice the tip radius r , the electric field has decayed to almost 10% of its initial value E_{\max} .

Figure 1(b) illustrates the analytical model used for the simulation of the lateral resolution of PFM. First, we define an active volume inside of which the electric field has decreased to a value E_{cut} which has to be identified later by fitting the experimental data. Beyond the active volume we set $E_z = 0$. The resulting piezomechanical deformation is calculated by integrating the contributions of the sample within the active volume:

$$\Delta z(x) = d_{33} z \int_{-E_{\text{cut}}}^{E_{\text{cut}}} \int_0^{E_{\text{cut}}} E_z(x, y, z) dE_y dE_z. \quad (2)$$

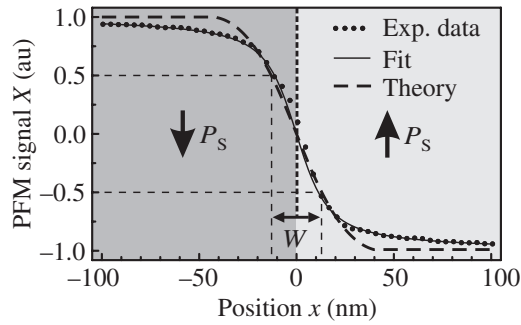


Figure 2. Measured PFM signal line scan perpendicular to a 180° domain wall in LiNbO_3 recorded with a tip of type B ($r = 15$ nm). The apparent domain wall width W is determined fitting the data using equation (3). For comparison, a line scan is shown that was calculated with the theoretical model for a tip of 15 nm radius. P_s denotes the orientation of the spontaneous polarization.

Here, $d_{33} = 8.1 \text{ pm V}^{-1}$ denotes the longitudinal piezoelectric coefficient for LiNbO_3 along the z -axis [20]. As can be seen in figure 1(b) the contributions of region I and III to the piezomechanical deformation cancel each other. For the simulation of the PFM signal when scanning across a domain wall, the active volume was subdivided into approx. 10^9 cubic elements. In order to determine E_{cut} the experimental data were fitted with the calculated slopes of the PFM signal across the domain wall. The best fits were obtained for $E_{\text{cut}} = 0.92 E_{\text{max}}$ for all tip radii. Note that the main assumption made for the simulation consists of the stiffness of the crystal, i.e. within a length of some microns the crystal parts cannot deform independently. The strength of clamping in bulk samples has been demonstrated by other experiments [22].

4. Experimental results

4.1. Dependence on the tip radius

In order to deduce the apparent domain wall width W from the experimental data, we normalized the PFM signals to an amplitude of 1 and fitted the data with a modified hyperbolic tangent

$$X(x) = A \tanh\left(\frac{x}{w}\right) + B \arctan\left(\frac{x}{w}\right), \quad (3)$$

where A , B and w are used as free parameters. Note that this function is only used to determine the width W but has no direct physical meaning. Then we applied a 25–75% criterion on the scan lines of the PFM signal which corresponds to the full width at half maximum of the PFM amplitude. Figure 2 shows an example for a measurement with a $r = 15$ nm tip on a LiNbO_3 sample. The measurement (dotted line) is fitted according to equation (3) (solid line). For comparison the slope of the PFM signal calculated with the analytical model is also depicted (dashed line). As can be seen, the error determining W using equation (3) is minimal therefore we do not show any error bars in the subsequent graphs.

On closer inspection of figure 2 one can see a discrepancy between measurement and theory at larger distances from the domain boundary. We attribute the broadening of the measured PFM line scans to the cone of the tip which is not taken into account in our analytical model. To reduce

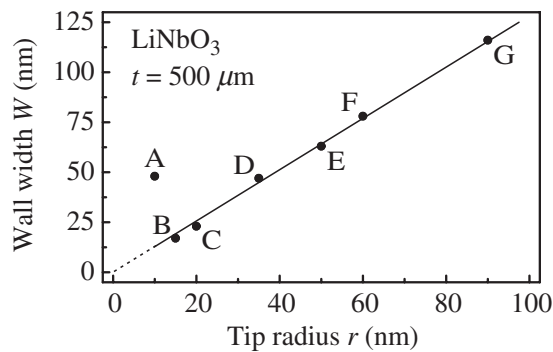


Figure 3. Measured domain wall width W as a function of the nominal tip radius r (comp. table 1). The straight line was calculated using the analytical model presented in this contribution. Note that despite its smaller radius, the uncoated tip A shows an inferior lateral resolution.

the influence of the cone on the determination of W we only consider the slope of the curves in a range similar to the tip radius. That is why we use the 25–75% criterion.

Processing the data in the above described manner, we extracted the data for W as a function of the tip radius as shown in figure 3. The straight line results from our analytical model. The excellent agreement between measurement and model is striking and strongly sustains the model to give reasonable estimates on W . Implicit to our model, an atomically sharp domain wall is thus also sustained by the PFM measurements. Note that with tip B a width of only 17 nm was measured, the smallest value recorded with PFM in bulk materials so far. This can be compared with a recent publication, where the lowest limit for W of 65 nm was estimated for LiNbO₃ [23]. That value as well as our currently highest resolution is by no means a fundamental limit of the material itself but of the available tip sizes. It is furthermore evidently seen that the non-coated tip A shows a substantially inferior lateral resolution ($W \approx 50$ nm) than expected by its tip radius of only 10 nm. This, however, is exactly what can be expected from a surface oxide layer: the conductive part of the tip being at a distance of several nanometres from the sample surface, separated by a dielectric SiO₂ layer generates a less localized electrical field inside the crystal, which results in a reduced spatial resolution.

4.2. Dependence on the sample thickness

In a further series of experiments, we determined W as a function of the sample thickness t varying the latter by three orders of magnitude from 0.9–1000 μm (figure 4). We used tips of type D with a nominal radius $r = 35$ nm. The accuracy and durability of the tips were controlled by measuring a standard 500 μm thick PPLN sample before and after each data acquisition with a sample of modified thickness. From figure 4 no change of the apparent width W within the thicknesses range of the samples could be observed. This, however, is consistent with our theoretical model where the electric field distribution E_z is found to be independent on the sample thickness t for $t > 15r$. In the case of tip D with a nominal radius of $r = 35$ nm the electric field E_z is thus the same for samples with thicknesses $t > 500$ nm.

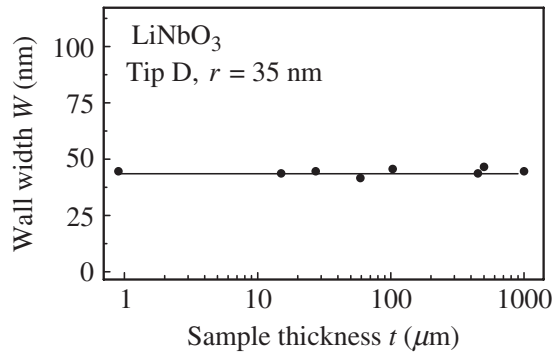


Figure 4. Measured domain wall width W as a function of sample thickness t . The straight line is the result from the analytical model.

Table 2. Apparent domain wall width W measured for different samples with tips of type B ($r = 15$ nm) and D ($r = 35$ nm). c–LiNbO₃: congruently melting and s–LiNbO₃: stoichiometric lithium niobate, respectively, SBN: Sr_{0.61}Ba_{0.39}Nb₂O₆. The last column lists the references for the values of the dielectric constants.

Sample	Domain wall width W (nm)		Dielectric anisotropy $\gamma = \sqrt{\varepsilon_z/\varepsilon_r}$	Reference
	$r = 15$ nm/ $r = 35$ nm			
BaTiO ₃	19/46		$0.17 = \sqrt{129/4380}$	[24]
KNbO ₃	18/45		$0.34 = \sqrt{44/384}$	[25]
c–LiNbO ₃	17/46		$0.58 = \sqrt{27.8/84.5}$	[20]
s–LiNbO ₃	17/45		0.58	[20]
Mg : LiNbO ₃	18/47		0.58	[20]
LiTaO ₃	18/45		$1.09 = \sqrt{53/44}$	[26]
KTiOPO ₄	17/46		$1.17 = \sqrt{15.5/11.5}$	[27]
Pb ₅ Ge ₃ O ₁₁	18/45		$1.40 = \sqrt{39/20}$	[28]
SBN	18/48		$1.52 = \sqrt{470/204}$	[29]

4.3. Dependence on the sample type

Finally, we compared W for different crystals using tips of type B and D (table 1). We again checked the reliability of the recorded data by always taking comparative measurements with a standard PPLN sample. All samples show the same apparent width W for a specific tip of radius $r = 15$ or 35 nm within an error of ± 1 nm, although their dielectric anisotropy $\gamma = \sqrt{\varepsilon_z/\varepsilon_r}$ differ as listed in table 2.

This can be understood if we calculate the electrical field, e.g. with the method of image charges where we place the charge q at $(0, 0, -r)$. In contrast to the case of an infinite isotropic half-plane, characterized by a single dielectric constant, we need two image charges q' at $(0, 0, r)$ and \tilde{q} at $(0, 0, \tilde{r})$ to account for the dielectric anisotropy given by ε_z and ε_r . The potential distribution above the surface is identical to the isotropic case but inside the crystal

it is given by

$$\varphi(x, y, z) = \frac{\tilde{q}}{\sqrt{\varepsilon_r^2 \varepsilon_z}} \frac{1}{\sqrt{(x^2 + y^2) / \varepsilon_r + (z - \tilde{r})^2 / \varepsilon_z}}. \quad (4)$$

The only way to satisfy the boundary conditions at the surface $(x, y, 0)$ is to set $\tilde{r} = \gamma r$ which leads to

$$E_z(x, y, z) = \frac{2q\gamma}{1 + \varepsilon_{\text{eff}}} \frac{z + r}{[x^2 + y^2 + (z + r)^2]^{3/2}}. \quad (5)$$

From this equation, we can clearly see that the dielectric anisotropy does not affect the shape of the electrical field distribution but only the field strength.

5. Conclusions

To summarize, we have analyzed the impact of the tip radius and the sample thickness on the apparent domain wall width W observed with PFM. We introduced an analytical model which explains the experimental data: a linear dependency of W on the tip radius as well as no dependency of W on the sample thickness as long as the sample is thicker than 15-times the tip radius. The model assuming an infinitely sharp domain wall is perfectly consistent with the experimental data. Furthermore, we carried out a series of measurements for different kinds of single crystals. Even though their material parameters differ significantly all measured domain wall widths were found to be independent of the specific sample. This is explained by the identical shape of the electrical field inside the sample, which is the basis of our analytical model.

Acknowledgments

We thank L Tian and V Gopalan for fruitful discussions. Many thanks to B Sturman for his steady support in theoretical concerns. We thank G Baldenberger from the Institut National d'Optique (Canada) for providing the PPLN samples, D Rytz from the Forschungsinstitut für mineralische und metallische Werkstoffe (Germany) for providing the BaTiO₃ and KNbO₃ samples, and the crystal growing team from the university of Osnabrueck for the Pb₅Ge₃O₁₁ sample. Financial support of the DFG research unit 557 and of the Deutsche Telekom AG is gratefully acknowledged.

References

- [1] Eason R W, Boyland A S, Mailis S and Smith P G R 2001 *Opt. Commun.* **197** 201
- [2] Fejer M M, Magel G A, Jundt D H and Byer R L 1992 *IEEE J. Quantum Electron.* **28** 2631
- [3] Ilchenko V S, Savchenkov A A, Matsko A B and Maleki L 2004 *Phys. Rev. Lett.* **92** 043903
- [4] Broderick N G R, Ross G W, Offerhaus H L, Richardson D J and Hanna D C 2000 *Phys. Rev. Lett.* **84** 4345
- [5] Cho Y, Hashimoto S, Odagawa N, Tanaka K and Hiranaga Y 2005 *Appl. Phys. Lett.* **87** 232907
- [6] Padilla J, Zhong W and Vanderbilt D 1996 *Phys. Rev. B* **53** R5969
- [7] Meyer B and Vanderbilt D 2002 *Phys. Rev. B* **65** 104111
- [8] Catalan G, Scott J F, Schilling A and Gregg J M 2007 *J. Phys.: Condens. Matter* **19** 022201
- [9] Yang T J, Gopalan V, Swart P J and Mohideen U 1999 *Phys. Rev. Lett.* **82** 4106

- [10] Dierolf V, Sandmann C, Kim S, Gopalan V and Polgar K 2003 *J. Appl. Phys.* **93** 2295
- [11] Foeth M, Sfera A, Stadelmann P and Buffat P-A 1999 *J. Electron Microsc.* **48** 717
- [12] Cho Y 2005 *Ferroelectric Thin Films (Top. Appl. Phys. vol 98)* ed M Okuyama and Y Ishibashi (New York: Oxford University Press) p 105
- [13] Newnham R E 2005 *Properties of Materials* (New York: Oxford University Press)
- [14] GÜthner P and Dransfeld K 1992 *Appl. Phys. Lett.* **61** 1137
- [15] Alexe M and Gruverman A (ed) 2004 *Nanoscale Characterisation of Ferroelectric Materials* 1st edn (Berlin: Springer)
- [16] Jungk T, Hoffmann A and Soergel E 2006 *Appl. Phys. Lett.* **89** 163507
- [17] Jungk T, Hoffmann A and Soergel E 2007 *J. Microsc.* **227** 72
- [18] Allik H and Hughes T J R 1970 *Int. J. Numer. Methods Eng.* **2** 151
- [19] Tian L, Capek P, Choudhury S, Eliseev E A, Morozovska A N, Dierolf V, Chen L, Kalinin S and Gopalan V to be published
- [20] Jazbinšek M and Zgonik M 2002 *Appl. Phys. B* **74** 407
- [21] Greiner W 2002 *Klassische Elektrodynamik* (Frankfurt am Main: Harri Deutsch Verlag)
- [22] Jungk T, Hoffmann A and Soergel E 2007 *J. Appl. Phys.* **102** 084102
- [23] Rodriguez B J, Nemanich R J, Kingon A, Gruverman A, Kalinin S V, Terabe K, Liu X Y and Kitamura K 2005 *Appl. Phys. Lett.* **86** 012906
- [24] Zgonik M, Bernasconi P, Duelli M, Schlessler R, Günter P, Garrett M H, Rytz D, Zhu Y and Wu X 1994 *Phys. Rev. B* **50** 5941
- [25] Zgonik M, Schlessler R, Biaggio I, Voit E, Tscherry J and Günter P 1993 *J. Appl. Phys.* **74** 1287
- [26] Kovacs G, Anhorn M, Engan H E, Visintini G and Ruppel C C W 1990 *Ultrason. Symp.* 435
- [27] Chu D K T, Bierlein J D and Hunsperger R G 1992 *IEEE Trans. Ultrason. Ferroelectr. Freq. Control* **39** 683
- [28] Mendricks S 1999 *Herstellung und Eigenschaften dotierter und thermisch behandelter $Pb_5Ge_3O_{11}$ Kristalle* (Aachen: Shaker Verlag)
- [29] Neurgaonkar R R, Oliver J R and Cross L E 1984 *Ferroelectrics* **56** 31